Bayesian Model Averaging for Estimating the Temperature Distribution in a Steam Methane Reforming Furnace

Anh Tran[1], Madeleine Pont[1], Andres Aguirre[1], Helen Durand[1], Marquis Crose[1] and Panagiotis D. Christofides[1,2]

[1] Department of Chemical & Biomolecular Engineering, University of California, Los Angeles
[2]Department of Electrical Engineering, University of California, Los Angeles

Inaugural Data Science Workshop

August 7, 2018

Uses and Applications of Hydrogen Gas

- Hydrogen is one of the most important raw materials for the petroleum refinery industry (Gupta, *CRC Press*, 2008)
  - Olefins $+H_2\,(g) \longrightarrow$ Paraffins
  - $R_1 - H_2C - CH_2 - R_2\,(g) + H_2\,(g) \longrightarrow R_1 - H_2CH\,(g) + HCH_2 - R_2\,(g)$
  - $R - SH\,(g) + H_2\,(g) \longrightarrow R\,(g) + H_2S\,(g)$

- Hydrogen is a precursor for many chemical industries, e.g., ammonia production
  - $3H_2\,(g) + N_2\,(g) \xrightarrow{\Delta H \ll 0} NH_3\,(g)$

- Hydrogen is a carrier gas for the production of thin film solar cells (Crose et al., *Chem. Eng. Science* , 2015)
  - $e^- + H_2\,(g) \longrightarrow e^- + 2H^\bullet$
  - $H^\bullet + SiH_4\,(g) \longrightarrow H_2\,(g) + (SiH_3)^\bullet$

- Hydrogen is an efficient energy carrier for hydrogen-based technologies (e.g. fuel cells)

General Information of Hydrogen Production

- In industry, hydrogen is produced by
  - Steam methane reforming (SMR) process, which accounts for 48% of world-wide hydrogen production (Ewan and Allen, *Int. J. Hydrogen Energy*, 2005)

$$CH_4(g) + H_2O(g) \underset{\substack{\Delta H \gg 0 \\ NiAl_2O_3}}{\rightleftharpoons} CO(g) + CO_2(g) + H_2(g) \qquad (1)$$

  - Top-fired reformer

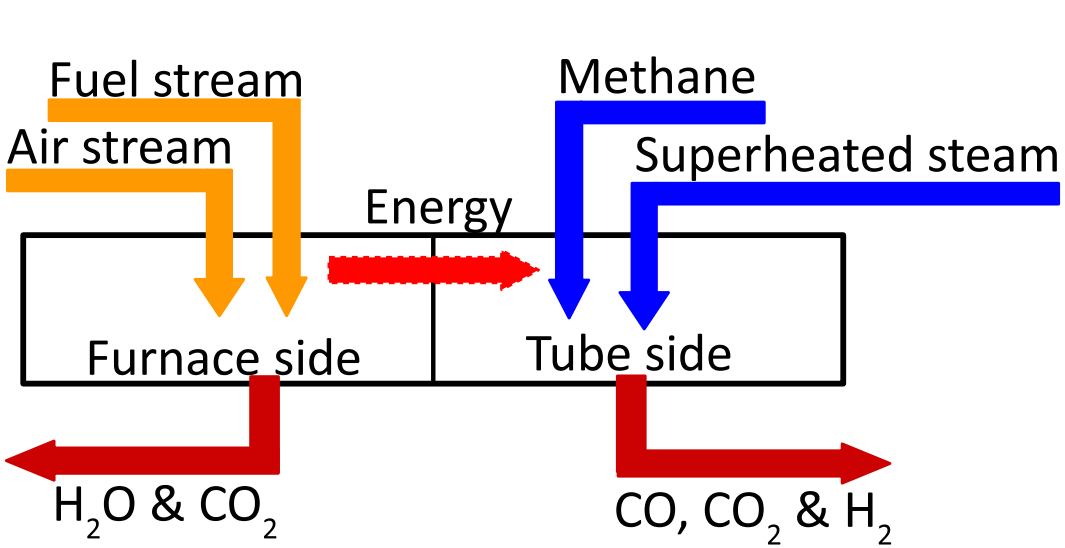

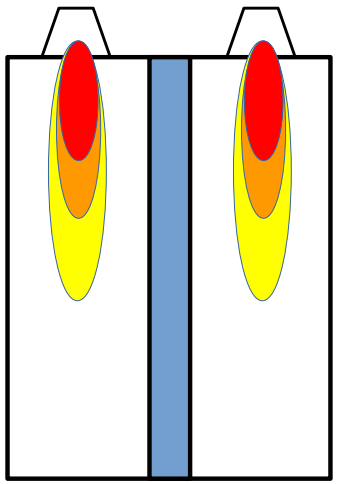
Top-fired reformer

Industrial-scale Steam Methane Reformer

- Geometry
  - Length: 16 m
  - Width: 16 m
  - Height: 13 m
- Components
  - 336 reforming tubes
  - 96 burners
  - 8 flue-gas tunnels
- Daily hydrogen production of 2.8×10^6 Nm^3
- Daily superheated steam production of 1.7×10^6 kg
- Annual operating cost of $\$62 \times 10^6$

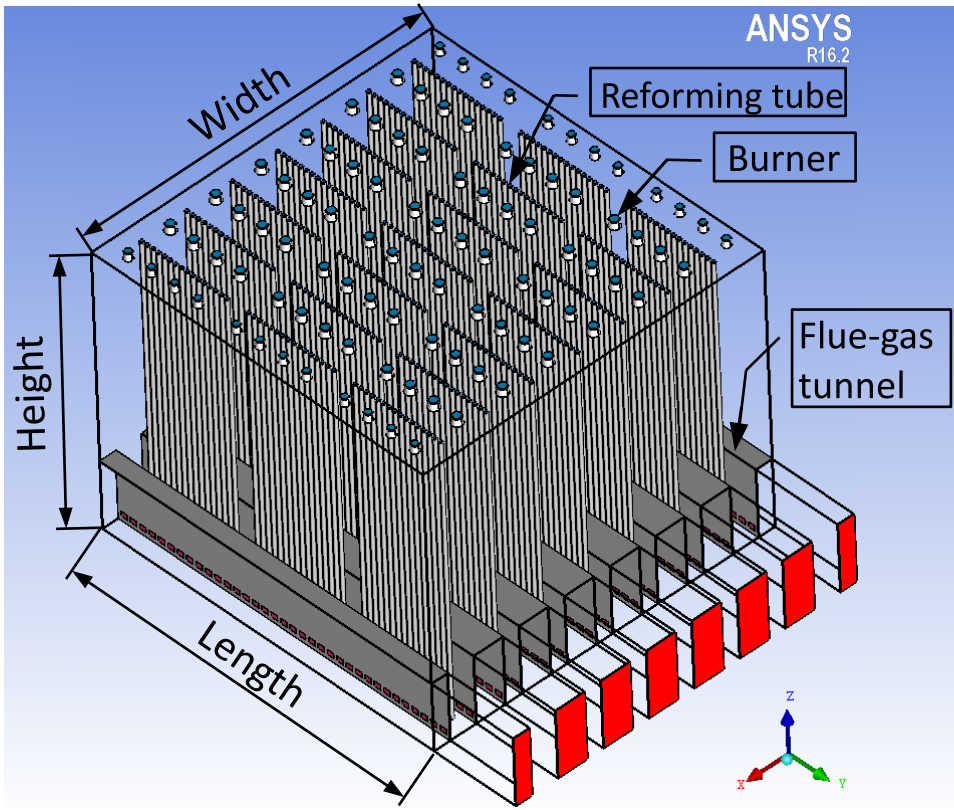

Industrial-scale Steam Methane Reformer Mesh

- The industrial-scale reformer mesh consists of 41 million grids

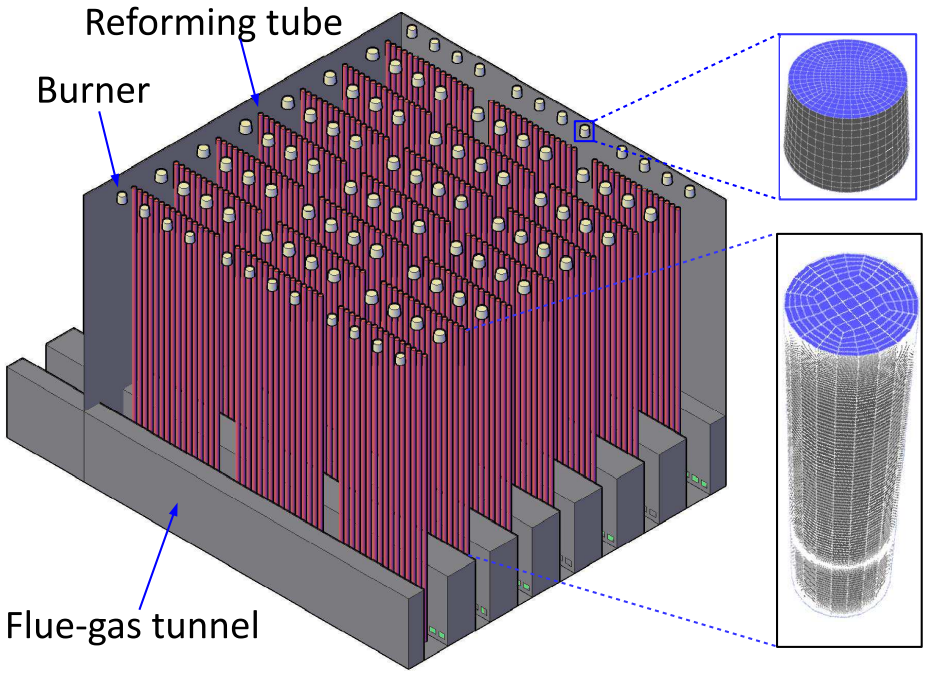

- Mesh information

	The reformer mesh	Recommended range
Min orthogonal factor	0.459	0.167 – 1.000
Max ortho skew	0.541	0.000 – 0.850

Industrial-scale Reformer CFD Model

- Modeling turbulent flows
  - Standard $k - \epsilon$ model with ANSYS enhanced wall treatment
- Modeling the combustion phenomena
  - Premixed combustion assumption
  - Global kinetic model of CH_4 combustion (D. G. Nicol, *PhD Thesis*, 1995)
  - Global kinetic model of H_2 combustion (Bane et al., *Technical Report*, 2010)
  - FR/ED turbulence-chemistry interaction model
- Modeling thermal radiation
  - Empirical model for radiative properties (A. Maximov, *PhD Thesis*, 2012)
  - Beer's law and Kirchoff's law
  - Discrete ordinate method

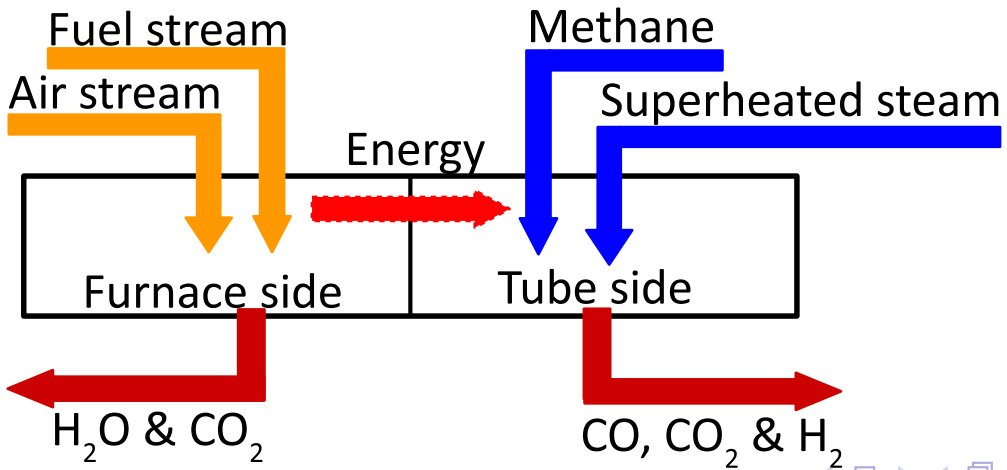

Industrial-scale Reformer CFD Model

- Modeling turbulent flows
  - Standard $k - \epsilon$ model with ANSYS enhanced wall treatment
- Modeling the catalyst network of each reforming tube
  - A continuum approach using ANSYS porous zone function
  - Effectiveness factor and catalyst packing factor
- Modeling the tube wall of each reforming tube
  - ANSYS thin wall function
- Modeling the SMR process
  - Global kinetic model (J. Xu and G. F. Froment, *AIChE Journal*, 1989)

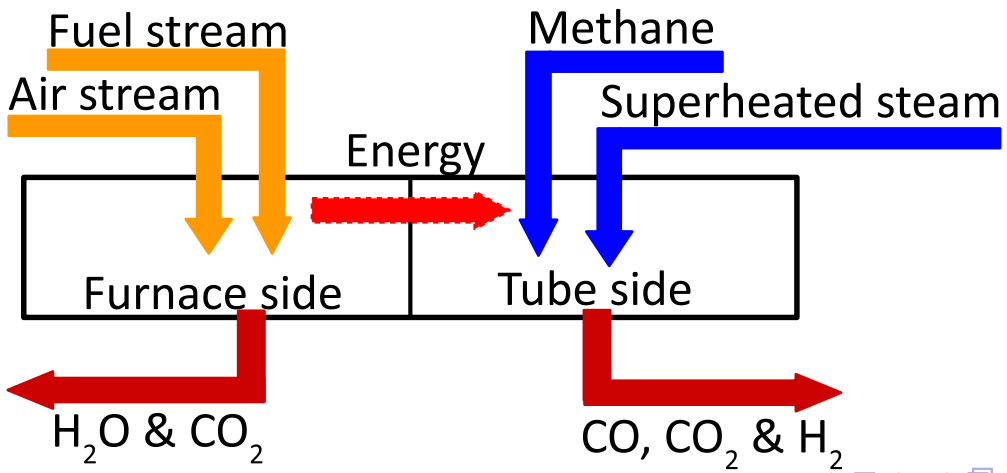

CFD Model Validation with Plant Data

- Simulation data generated by the reformer CFD model is in good agreement with the data provided by industry

	Reformer CFD model	Industry	Deviation
Fired duty (kW)	209474.8	211597.3	1.0 %
Total absorbed heat (kW)	113895.5	112246.2	1.5%
Fraction of absorbed heat (%)	54.4	53.1	2.4%
OD average heat flux (kW/m^2)	59.2	58	2.1%
ID average heat flux (kW/m^2)	69.5	75.7	8.2%
Average outlet flue gas temp (K)	1243.1	1283	3.1%
$\bar{x}_{H_2}^{outlet}$	46.5	46.8	0.6 %

Motivations for Data-driven Modeling

- The reformer service life is monitored by the system of infrared cameras that periodically record the outer wall temperatures (OTWTs) of the reforming tubes in real-time
- Feedback from our third-party collaborator and publicly available literature suggest that OTWTs can be controlled by the total fuel flow rate and its spatial distribution inside the reformer
- We developed an integrated model identification procedure to discover the dependence of the OTWT distribution on the reformer input using
  - Bayesian variable selection
  - Sparse nonlinear regression
  - Bayesian model averaging
  - Theories of thermal radiation
  - Reformer geometry

Data-driven Model for the *ith* OTWT

- The data-driven model for the relationship between the i^{th} OTWT at a fixed height and the furnace-side feed (FSF) distribution is formulated as follows,

$$\widehat{T}_i^{P,n} = \sum_{k=1}^{K_i} w_{i,k}^P \widetilde{T}_{i,k}^{P,n} \tag{2a}$$

where

$$\sum_{k=1}^{K_i} w_{i,k}^P = 1 \tag{2b}$$

$$\widetilde{T}_{i,k}^{P,n} = \sum_{g=1}^{G} \left(\vec{\alpha}_i^{kg}\right)^T \cdot f_g\left(\vec{F}^n\right) + \alpha_i^k \tag{2c}$$

$$\vec{F}^n = \left[F_1^n, F_2^n, \cdots, F_{96}^n\right]^T \tag{2d}$$

$$\left\|\vec{F}^n\right\|_1 = F_{tot}^n \tag{2e}$$

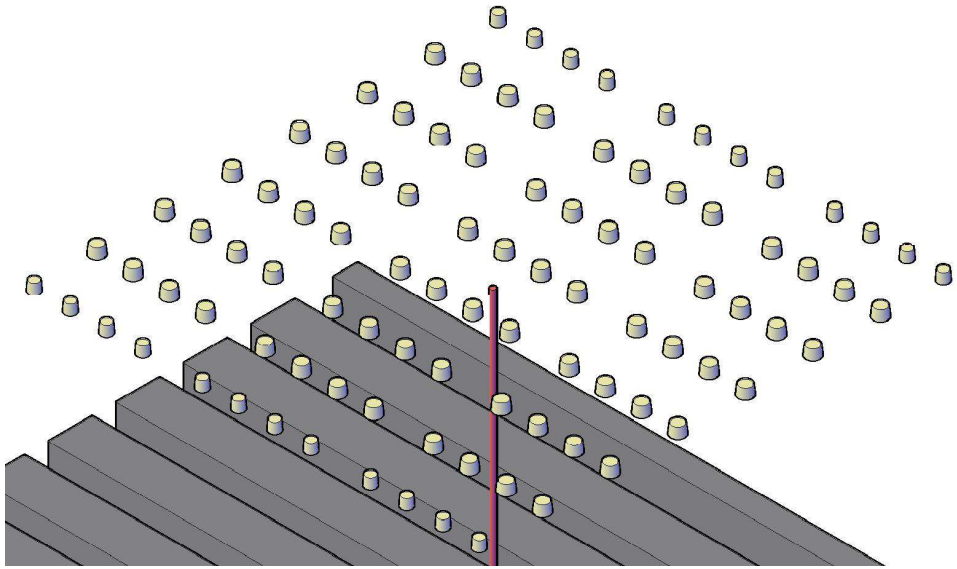

- $\widehat{T}_i^{P,n}$ is the BMA estimate of the *ith* OTWT
- $\widetilde{T}_{i,k}^{P,n}$ is the estimate of the *ith* OTWT based on the *kth* sub-model for the *ith* OTWT
- $f_g\left(\vec{F}^n\right)$ is the *gth* basis function in the library of transformation functions

k^{th} Sub-model for the *ith* OTWT (i.e., $M_{i,k}$)

$$\widetilde{T}_{i,k}^{P,n} = \sum_{g=1}^{G} \left(\vec{\alpha}_i^{kg}\right)^T \cdot f_g\left(\vec{F}^n\right) + \alpha_i^k \tag{3}$$

where

$$f_1\left(\vec{F}^n\right) = \left[F_1^n, F_2^n, \cdots, F_{96}^n\right]^T$$

$$f_2\left(\vec{F}^n\right) = \left[\left(F_1^n\right)^2, \left(F_2^n\right)^2, \cdots, \left(F_{96}^n\right)^2\right]^T$$

$$f_3\left(\vec{F}^n\right) = \left[\left(F_1^n\right)^3, \left(F_2^n\right)^3, \cdots, \left(F_{96}^n\right)^3\right]^T$$

$$f_4\left(\vec{F}^n\right) = \left[\sqrt[2]{F_1^n}, \sqrt[2]{F_2^n}, \cdots, \sqrt[2]{F_{96}^n}\right]^T$$

$$f_5\left(\vec{F}^n\right) = \left[\sqrt[3]{F_1^n}, \sqrt[3]{F_2^n}, \cdots, \sqrt[3]{F_{96}^n}\right]^T$$

$$f_6\left(\vec{F}^n\right) = \left[\sqrt[4]{F_1^n}, \sqrt[4]{F_2^n}, \cdots, \sqrt[4]{F_{96}^n}\right]^T$$

$$f_7\left(\vec{F}^n\right) = \left[\sqrt[5]{F_1^n}, \sqrt[5]{F_2^n}, \cdots, \sqrt[5]{F_{96}^n}\right]^T$$

$$f_8\left(\vec{F}^n\right) = \left[\exp\left(F_1^n\right), \exp\left(F_2^n\right), \cdots, \exp\left(F_{96}^n\right)\right]^T$$

- $G = 8$ is the number of functions in the library of transformation functions
- $\vec{\alpha}_i^{kg} \in \mathbb{R}^{96\times 1}$ is the empirical vector of $M_{i,k}$ corresponding to $f_g(\cdot)$
- $\alpha_i^k \in [298.15, 348.15]$ is the estimated ambient temperature of $M_{i,k}$

Spare Nonlinear Regression with MLE

- The formulation for the sparse nonlinear regression with MLE is proposed as follows

$$\min_{\substack{\alpha_i^k \in [298.15, 348.15] \\ \alpha_{ij}^{kg} \in [0,\infty)}} \sum_{n=1}^{N} \frac{\left(T_i^n - \widetilde{T}_{i,k}^{P,n}\right)^2}{2\left(\sigma_i^n\right)^2} + \lambda_i \sum_{g=1}^{8} \left\| \vec{\alpha}_i^{kg} \right\|_1 \tag{6}$$

subject to

$$\sum_{g=1}^{8} \alpha_{il}^{kg} f_g\left(\overline{F}^0\right) = \sum_{g=1}^{8} \alpha_{ij}^{kg} f_g\left(\overline{F}^0\right) \quad \text{if } d_{il} = d_{ij} \tag{7a}$$

$$\sum_{g=1}^{8} \alpha_{il}^{kg} f_g\left(\overline{F}^0\right) \geq \left(\frac{d_{ij}}{d_{il}}\right)^{\beta_l} \sum_{g=1}^{8} \alpha_{ij}^{kg} f_g\left(\overline{F}^0\right) \quad \text{if } d_{il} < d_{ij} \tag{7b}$$

$$\sum_{g=1}^{8} \alpha_{il}^{kg} f_g\left(\overline{F}^0\right) \leq \left(\frac{d_{ij}}{d_{il}}\right)^{\beta_u} \sum_{g=1}^{8} \alpha_{ij}^{kg} f_g\left(\overline{F}^0\right) \quad \text{if } d_{il} < d_{ij} \tag{7c}$$

$$\overline{F}^0 = \frac{F_{tot}^{typ}}{96} \tag{7d}$$

Spare Nonlinear Regression with MLE

- Regressors of the *ith* OTWT are defined as the burners that directly control the *ith* OTWT

$$\widetilde{T}_{i,k}^{P,n} = \sum_{g=1}^{G} \left(\hat{\vec{\alpha}}_i^{kg} \right)^T \cdot f_g \left(\vec{F}^n \Big|_{S_{iR}} \right) + \hat{\alpha}_i^k \qquad (8)$$

- $S_{iR} \in \mathbb{R}^{j \times 1}$ is the given set of regressors
- $\hat{\vec{\alpha}}_i^{kg}$ is the MLE of $\vec{\alpha}_i^{kg} \in \mathbb{R}^{j \times 1}$
- $\hat{\alpha}_i^k$ is the MLE of $\alpha_i^k \in \mathbb{R}$
- $\vec{F}^n \Big|_{S_{iR}} \in \mathbb{R}^{j \times 1}$ is the design matrix

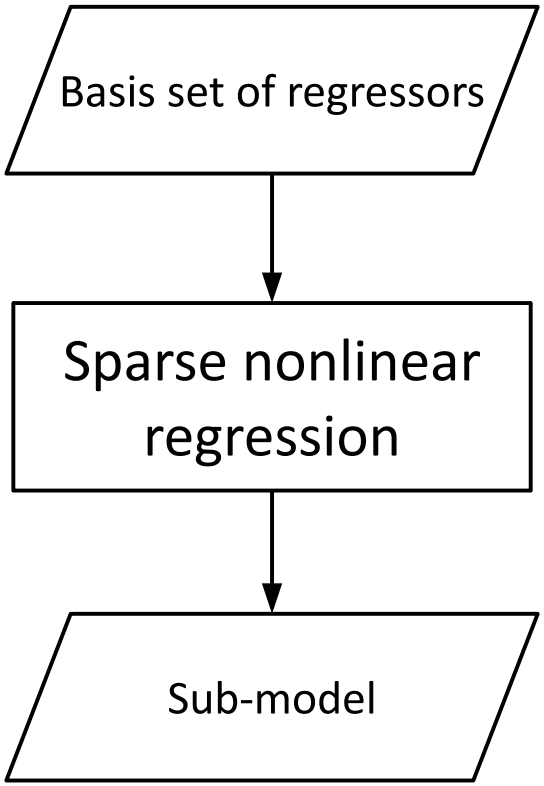

Model Identification Flow Diagram

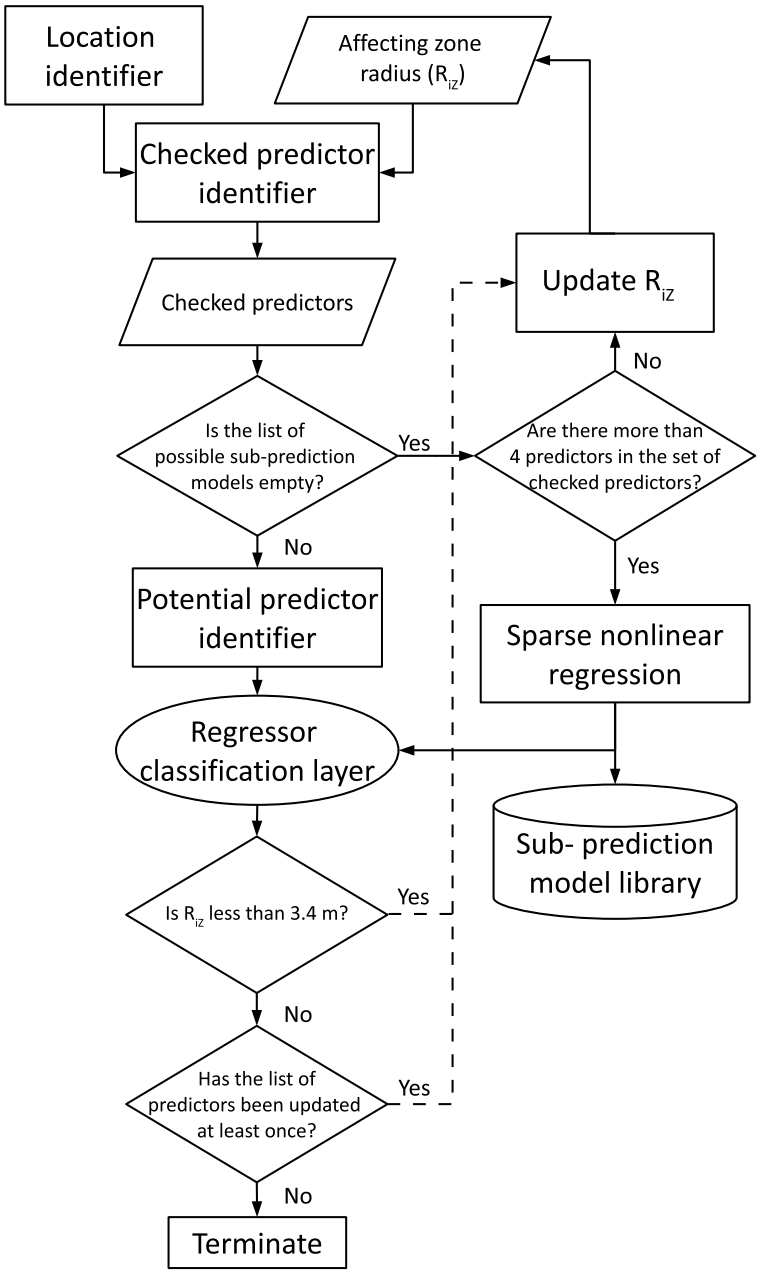

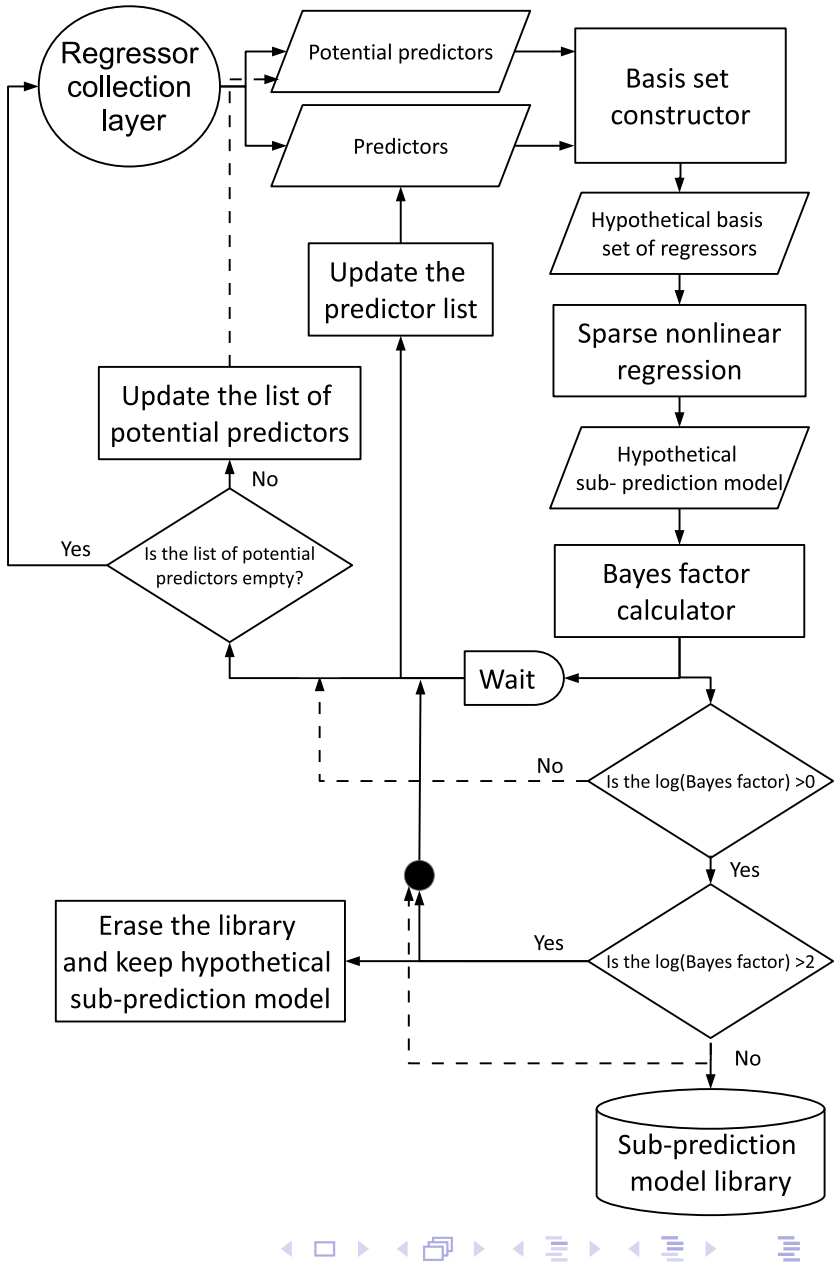

Simulation Inputs

- 21 reformer CFD data sets with varying FSF distributions and total FSF flow rates are available
- Reformer CFD data sets are partitioned into two categories
  - A reformer CFD training data consists of 18 data sets
  - A reformer CFD testing data consists of 3 data sets
- $\mathbf{S}_\lambda = \{0.1, 0.2, \cdots, 1.0, 1.2, \cdots, 2.0, 5.0, 10, 20\}$, which controls the model complexity and goodness of fit
  - Small values of λ_i result in a low degree of shrinkage and favor overfitting data-driven models with high goodness of fit
  - Large values of λ_i result in a high degree of shrinkage and favor underfitting data-driven models with low levels of complexity
- Leave-one-out cross validation is used to find the best λ_i
- The 77*th* reforming tube is chosen as a representative example because the number of sub-models with high goodness of fit (i.e., 4) and the number of predictors (i.e., 9) for the 77*th* OTWT

Results

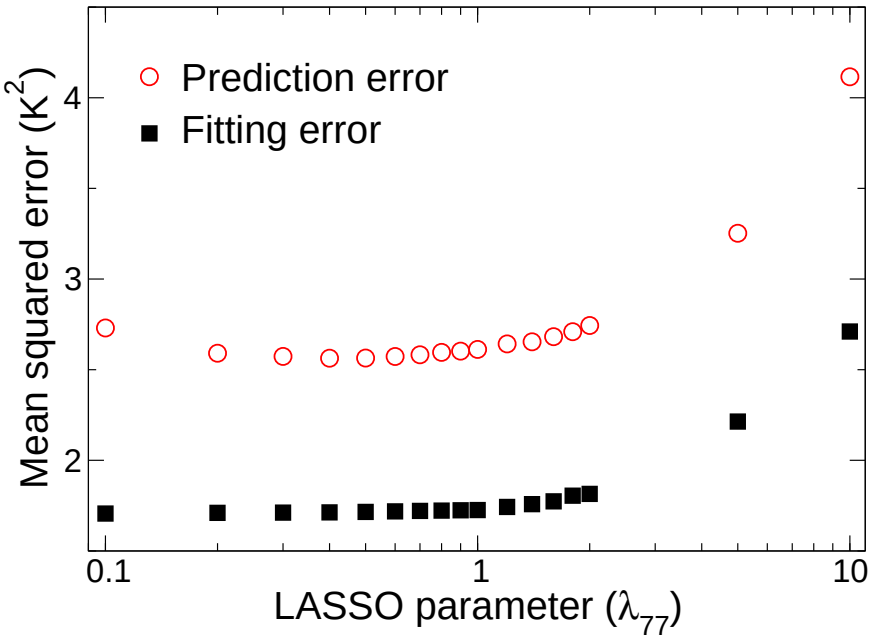

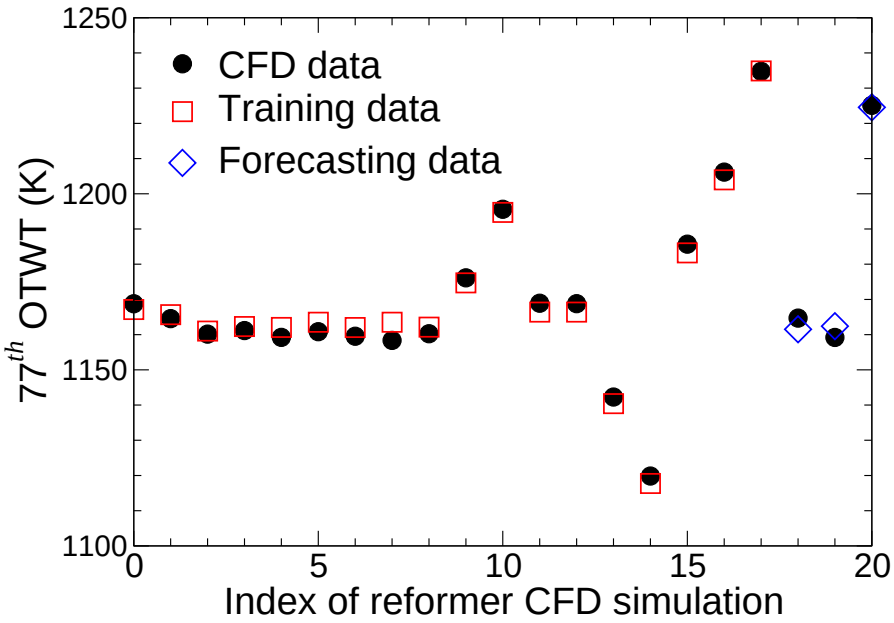

- The smallest fitting error corresponds to the smallest value of λ=0.1
- The largest fitting error corresponds to the largest value of λ=10
- The smallest prediction error corresponds to $\widehat{\lambda_{77}}$=0.5

- The model for the 77*th* OTWT

$$\widehat{T}_{77}^{P,n} = 0.01\widetilde{T}_{77,1}^{P,n} + 0.23\widetilde{T}_{77,2}^{P,n} + 0.29\widetilde{T}_{77,3}^{P,n} + 0.47\widetilde{T}_{77,4}^{P,n} \quad (9)$$

Results

- The data-driven model for the OTWT distribution correctly identifies the hot and cold regions
- The absolute maximum and average deviations from the reformer CFD data are 20.1 K and 2.9 K, respectively

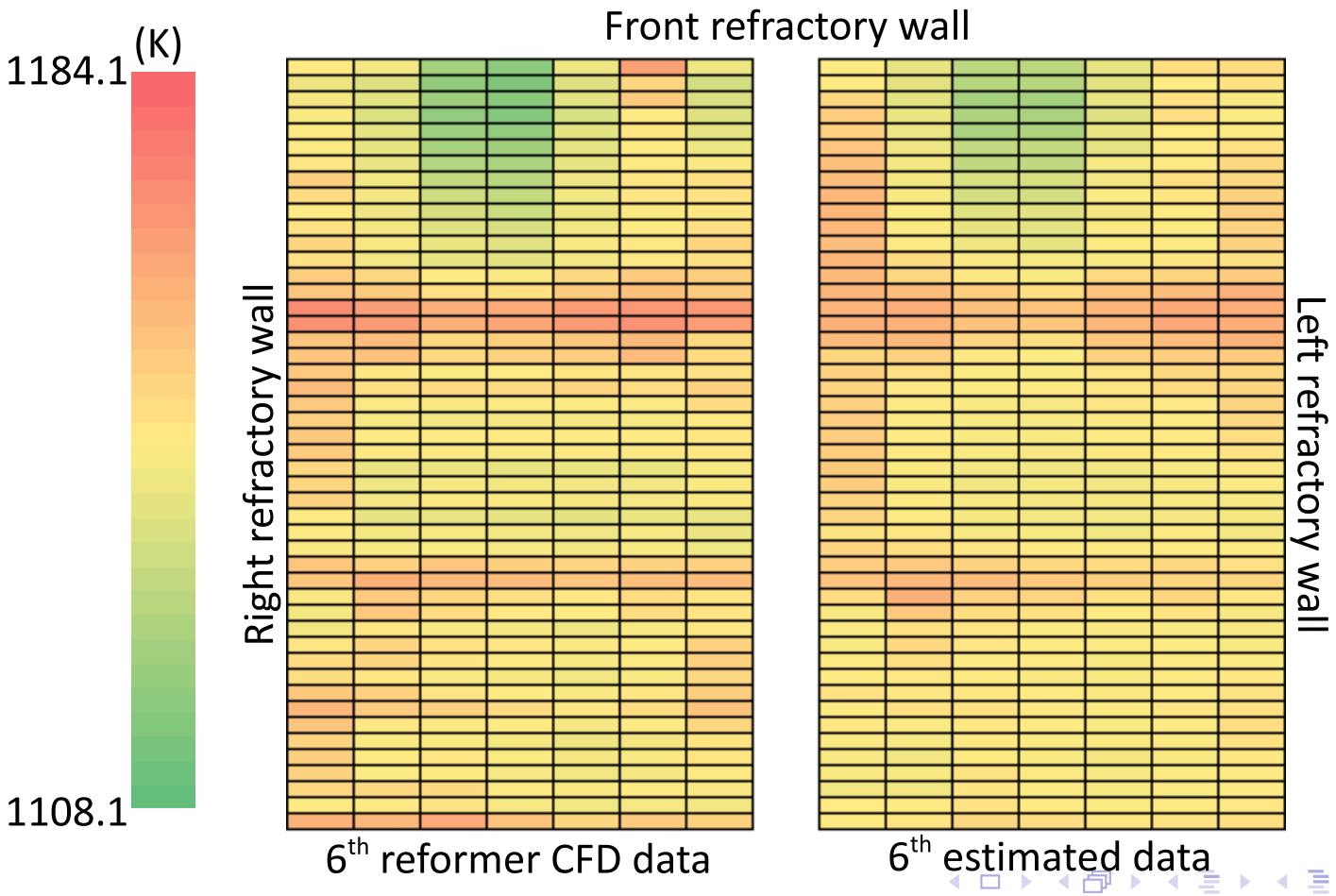

Flowchart of The Furnace-balancing Scheme

- The furnace-balancing scheme is developed based on
  - The high-fidelity reformer CFD model (Tran et al., *Chem. Eng. Sci.*, 2017)
  - The statistical-based model identification (Tran et al., *Chem. Eng. Res. Des.*, in press)
  - The furnace-balancing optimizer (Tran et al., *Comp. & Chem. Eng.*, 2017)

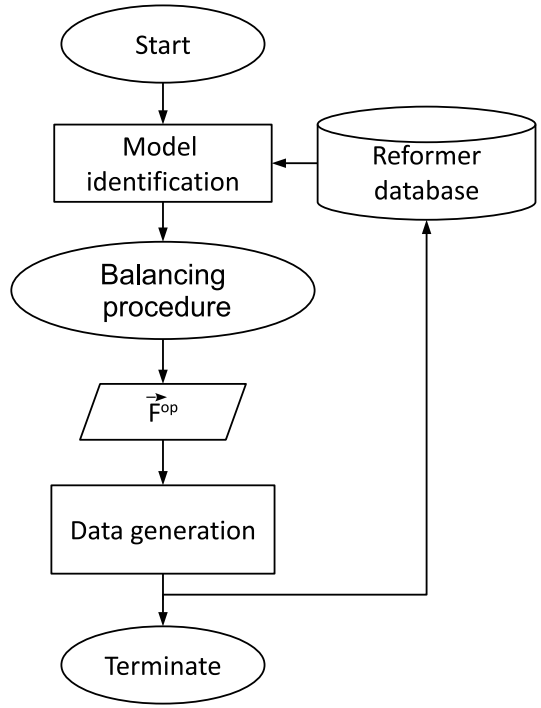

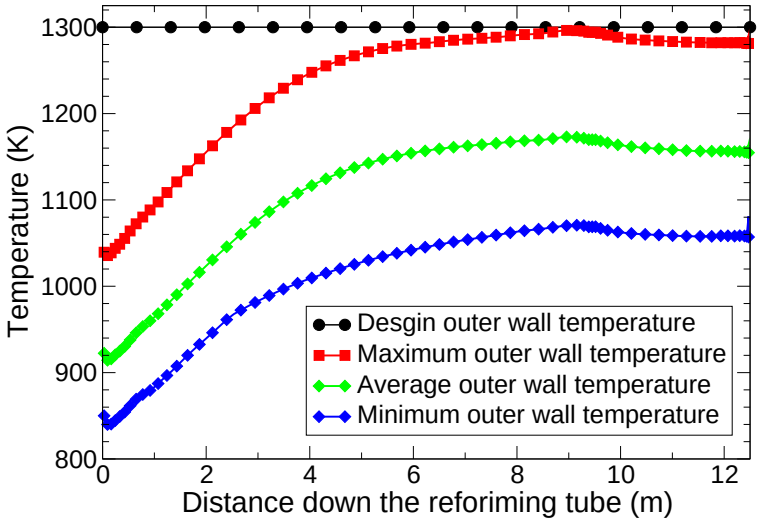

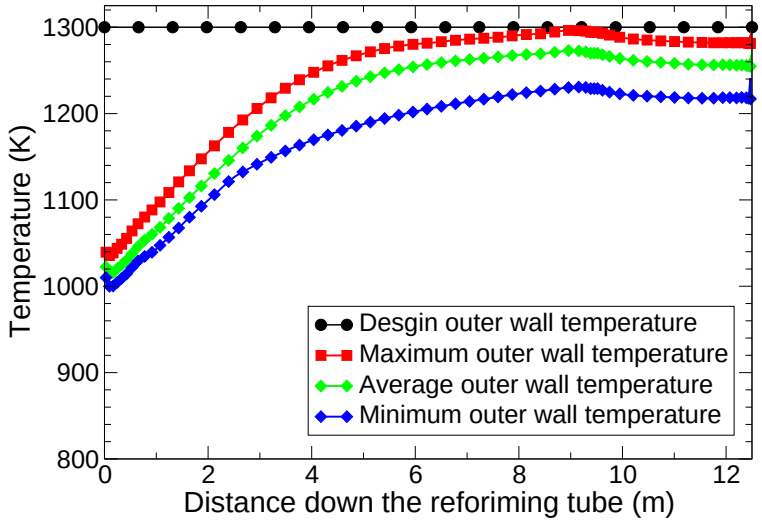

Results

- This result is obtained within a minute
- The total FSF flow rate is increased by 40% from 98.113 to 136.896 kg sec^{-1} without damaging the reforming tubes indicated by the evidence that the maximum value in the OTWT distribution is 1288.35 K

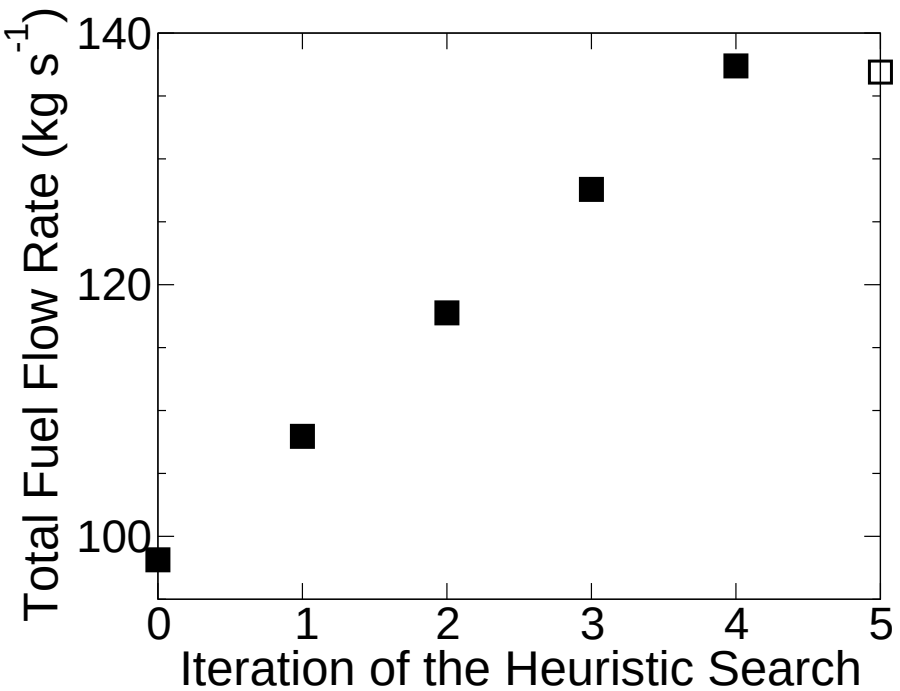

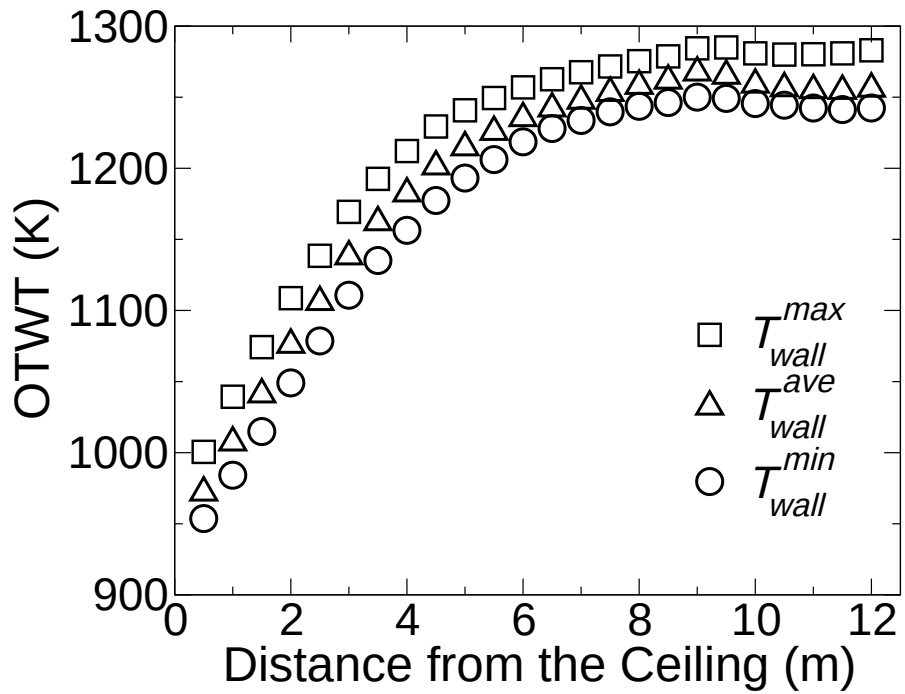

Conclusion

- The integrated model identification procedure is structured to be fully distributed, which allows the data-driven model for 336 reforming tubes to be derived simultaneously from the training data and independently from one another
- Leave-out-one cross validation is successfully implemented to find the optimal LASSO parameter for each reforming tube
- The results from the goodness-of-fit and out-of-sample prediction tests of the data-driven model for the OTWT distribution demonstrated the high effectiveness of the method proposed in this work

Acknowledgments

- Financial support from the Department of Energy is gratefully acknowledged